Capacity Bounds and Performance of Precoder Index Modulation

Yalagala Naresh, T. Lakshmi Narasimhan†, and A. Chockalingam
Department of ECE, Indian Institute of Science, Bangalore 560012
† Presently with National Instruments Private Limited, Bangalore 560029

***Abstract*—Precoder index modulation (PIM) is a recently proposed transmission scheme in which the index of the chosen precoder matrix from a set of predetermined pseudo-random phase precoder (PRPP) matrices will also convey information bits in addition to the information bits conveyed through conventional modulation symbols. In this paper, first we derive lower and upper bounds on the capacity of PIM. Second, since the optimum PIM detection has an exponential complexity in the precoder size, we propose a low complexity message passing based detection algorithm suited for large precoder sizes. Simulation results show that PIM with a precoder matrix of size 150×150 and BPSK achieves a BER of 10^{-5} at an SNR of about 10 dB using the proposed detection algorithm in flat Rayleigh fading channels. Third, we also propose an enhanced PIM (E-PIM) scheme which provides additional signaling support to the index bits, but without loosing spectral efficiency compared to PIM. Simulation results show that the proposed E-PIM scheme achieves better performance compared to PIM.**

Keywords – *Precoder index modulation, pseudo-random phase precoding, PIM capacity, message passing detection, enhanced PIM.*

I. INTRODUCTION

Index modulation schemes for communication are emerging as an interesting and promising area of research. Conventional modulation schemes convey information bits only through symbols from a chosen modulation alphabet like QAM/PSK. In index modulation, on the other hand, additional information bits are conveyed through the indices of certain transmit entities that get involved in the transmission. Spatial modulation (SM) is one example, where indexing is done in the spatial domain in multi-antenna systems [1],[2]. In SM, the index of the active antenna among the available transmit antennas conveys additional information bits. Another example is subcarrier index modulation, where indexing is done in the frequency domain in multi-carrier systems [3]-[5]. Here, additional bits are conveyed through the indices of active subcarriers. An advantage of index modulation over conventional modulation is that, to achieve a certain spectral efficiency, index modulation can use a smaller-sized QAM/PSK alphabet compared to that needed in conventional modulation. This, in turn, can lead to SNR gains (for a given probability of error performance) in favor of index modulation [6],[7]

The idea of conveying information bits through indices of precoder matrices – termed as precoder index modulation (PIM) – was first introduced in [8]. A basic ingredient in PIM is a set of predetermined pseudo-random phase precoder (PRPP) matrices. Precoding using a PRPP matrix has been shown to offer diversity benefits even in single-input single-output (SISO) fading channels without the need for channel state information at the transmitter (CSIT) [9]. Further, when the precoder sizes are large, one can achieve near-exponential diversity using suitable low complexity detection algorithms [9],[10]. PIM exploits this diversity benefit of precoding using PRPP matrices as well as the performance advantage of indexing these PRPP matrices. In PIM, additional information bits are conveyed through the choice of a precoding matrix from the set of PRPP matrices. The selected PRPP matrix is used to precode modulation symbols. It has been shown that PIM can outperform conventional systems with classical modulation (e.g., QAM, PSK) as well as PRPP system without precoder indexing [8], [11]. For example, in a SISO Rayleigh fading channel, at a spectral efficiency of 4 bpcu with 5×5-sized precoder matrices, PIM achieves an improved performance by about 2.5 dB at 10^{-3} BER compared to PRPP without precoder indexing. This is because, to achieve the same spectral efficiency of 4 bpcu, PRPP without precoder indexing uses 16-QAM, whereas PIM uses 4-QAM (to convey two bits per channel use) and 1024 PRPP matrices (to convey two more bits per channel use through indexing). This potential to achieve improved performance motivates further investigation of PIM, which forms the basic premise of this paper. In particular, this paper addresses the following two important questions related to PIM: i) what can we say about the capacity of PIM, and ii) how can we detect PIM signals with large precoder sizes. Our new contributions in this paper can be summarized as follows.

- First, we derive lower and upper bounds on the capacity of PIM and present numerical results on these bounds.
- Second, since the optimum PIM detection has an exponential complexity in the precoder size, we propose a low complexity message passing based detection algorithm suited for large precoder sizes. Simulation results show that PIM with a precoder matrix of size 150×150 and BPSK achieves a BER of 10^{-5} at an SNR of about 10 dB using the proposed algorithm in flat Rayleigh fading.
- Third, we propose an enhanced PIM (E-PIM) scheme which provides additional signaling support to the index bits, but without loosing spectral efficiency compared to PIM. Simulation results show that the proposed E-PIM scheme achieves better performance compared to PIM.

The rest of the paper is organized as follows. In Section II, we present the PIM system model. The bounds on PIM capacity are derived in Section III. The proposed detection algorithm for PIM with large precoder sizes is presented in Section IV. Section V presents the proposed enhanced PIM scheme. Conclusions are presented in Section VI.

II. PIM SYSTEM

The PIM transmitter is shown in Fig. 1. It uses a collection of precoder matrices each of size $p \times p$ and chooses one

This work was supported in part by the J. C. Bose National Fellowship, Department of Science and Technology, Government of India, and by the Indo-French Centre for Applied Mathematics.

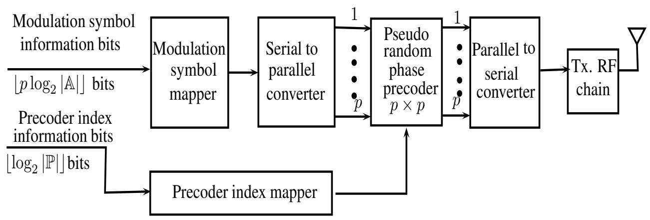

Fig. 1. PIM transmitter.

among these matrices to precode p modulation symbols from an modulation alphabet $\mathbb{A}$ in p channel uses. Let us call this collection of matrices as 'precoder set,' denoted by $\mathbb{P}$.

Construction of the precoder set: The precoder set $\mathbb{P} = \{\mathbf{P}_1, \mathbf{P}_2, \cdots, \mathbf{P}_{|\mathbb{P}|}\}$ is constructed as follows. Let n denote the number of precoder index bits per channel use, i.e., $n \triangleq \frac{1}{p}\lfloor \log_2|\mathbb{P}|\rfloor$. Generate a matrix $\mathbf{Q}$ of size $p \times pn_p$, where $n_p = 2^n$. The (r,c)th entry of the precoder matrix $\mathbf{Q}$ is $\frac{1}{\sqrt{p}}e^{\jmath\theta_{r,c}}$, where $\jmath = \sqrt{-1}$, and the phases $\{\theta_{r,c}\}$ are drawn from uniform distribution in $[0, 2\pi)$ using a pseudo-random sequence generator. The seed of this random number generator is pre-shared among the transmitter and receiver. Note that the precoder set size $|\mathbb{P}| = (n_p)^p$. The matrix $\mathbf{Q}$ can be written as

$$\mathbf{Q} = [\mathbf{Q}_1\ \mathbf{Q}_2\ \cdots\ \mathbf{Q}_p],$$

where $\mathbf{Q}_i$s are sub-matrices each of size $p \times n_p$. Now, a precoder matrix $\mathbf{P}_m$ of size $p \times p$, $m = 1, \cdots, |\mathbb{P}|$, is formed such that its ith column is drawn from the columns of $\mathbf{Q}_i$. $\mathbf{Q}_i$, $i = 1, \cdots, p$. Since there are n_p columns in each $\mathbf{Q}_i$, the number of matrices in the precoder set is $|\mathbb{P}| = (n_p)^p$.

Example 1: We illustrate the precoder set construction using the following example. Consider $p = 2$ and $n_p = 2$, and

$$\mathbf{Q} = [\mathbf{Q}_1\ \mathbf{Q}_2] = \Bigg[\underbrace{\begin{bmatrix} q_{11} & q_{12} \\ q_{21} & q_{22} \end{bmatrix}}_{\mathbf{Q}_1} \underbrace{\begin{bmatrix} q_{13} & q_{14} \\ q_{23} & q_{24} \end{bmatrix}}_{\mathbf{Q}_2}\Bigg]. \quad (1)$$

where q_{ij} denotes the (i,j)th element in $\mathbf{Q}$, i varies from 1 to p $(= 2)$, and j varies from 1 to pn_p $(= 4)$. The column indices for submatrix $\mathbf{Q}_i$ in $\mathbf{Q}$ vary from $(i-1)n_p+1$ to in_p. Now, as mentioned above, forming the precoder matrices $\mathbf{P}_m$, $m = 1, \cdots, 4$ by drawing columns from $\mathbf{Q}_1$ and $\mathbf{Q}_2$ in (1), the precoder matrix set obtained is given by

$$\mathbb{P} = \Bigg\{ \underbrace{\begin{bmatrix} q_{11} & q_{13} \\ q_{21} & q_{23} \end{bmatrix}}_{\mathbf{P}_1}, \underbrace{\begin{bmatrix} q_{11} & q_{14} \\ q_{21} & q_{24} \end{bmatrix}}_{\mathbf{P}_2}, \underbrace{\begin{bmatrix} q_{12} & q_{13} \\ q_{22} & q_{23} \end{bmatrix}}_{\mathbf{P}_3}, \underbrace{\begin{bmatrix} q_{12} & q_{14} \\ q_{22} & q_{24} \end{bmatrix}}_{\mathbf{P}_4} \Bigg\}. \quad (2)$$

PIM Transmitter: The transmitter (see Fig. 1) takes $p\lfloor \log_2|\mathbb{A}|\rfloor + \lfloor \log_2|\mathbb{P}|\rfloor$ bits and encodes them as follows. The $p\lfloor \log_2|\mathbb{A}|\rfloor$ bits are used to form p modulation symbols. Let $\mathbf{s} \in \mathbb{A}^p$ denote the vector of these modulation symbols. The transmitter selects a precoder matrix $\mathbf{P} \in \mathbb{P}$ using $\lfloor \log_2|\mathbb{P}|\rfloor$ additional bits. The selected $\mathbf{P}$ matrix is used to precode the the symbol vector $\mathbf{s}$. The precoded vector $\mathbf{Ps}$ is transmitted in p channel uses.

Precoder selection matrix: To select a precoder matrix $\mathbf{P}$ from the precoder set $\mathbb{P}$, a precoder selection matrix $\mathbf{A}$ of size $pn_p \times p$ consisting of 1s and 0s such that $\mathbf{P} = \mathbf{QA} \in \mathbb{P}$ is constructed. This $\mathbf{A}$ matrix is constructed using $\lfloor \log_2|\mathbb{P}|\rfloor = np$ bits as follows. $\mathbf{A}$ is formed using p submatrices $\mathbf{A}_{(i)}$, $i = 1, \cdots, p$, each of size $n_p \times p$, as $\mathbf{A} = [\mathbf{A}_{(1)}^T\ \mathbf{A}_{(2)}^T\ \cdots\ \mathbf{A}_{(p)}^T]^T$. The submatrix $\mathbf{A}_{(i)}$ is constructed as

$$\mathbf{A}_{(i)} = [\mathbf{0}_{(1)}\ \mathbf{0}_{(2)}\ \cdots\ \mathbf{0}_{(i-1)}\ \mathbf{a}_{(i)}\ \mathbf{0}_{(i+1)}\ \cdots\ \mathbf{0}_{(p)}], \quad (3)$$

where $\mathbf{0}_{(k)}$ is a $n_p \times 1$ vector of zeros, and $\mathbf{a}_{(i)}$ is a $n_p \times 1$ vector constructed as

$$\mathbf{a}_{(i)} = [0 \cdots 0 \underbrace{1}_{j_i\text{th coordinate}} 0 \cdots 0]^T, \quad (4)$$

where j_i is the index of column of $\mathbf{Q}_i$ chosen based on n bits. In other words, one n-bit block is used to obtain one submatrix of $\mathbf{A}$, so that the entire $\mathbf{A}$ matrix is obtained using np bits. The selected precoder matrix is then obtained as $\mathbf{P} = \mathbf{QA}$.

Example 2: The $\mathbf{A}$ matrix for selecting precoder matrix $\mathbf{P}_3$ from $\mathbb{P}$ given by (2) in *Example 1* can be obtained as follows. Note that the 1st column of $\mathbf{P}_3$ is the 2nd column of $\mathbf{Q}_1$, i.e., j_1 in (4) is 2. Likewise, since the 2nd column of $\mathbf{P}_3$ is the 1st column of $\mathbf{Q}_2$, j_2 in (4) is 1. Therefore, the $\mathbf{A}$ matrix is

$$\mathbf{A} = [\mathbf{A}_{(1)}^T\ \mathbf{A}_{(2)}^T]^T = \left[\begin{array}{cc|cc} 0 & 1 & 0 & 0 \\ 0 & 0 & 1 & 0 \end{array}\right]^T. \quad (5)$$

Note that multiplying $\mathbf{Q}$ in (1) with $\mathbf{A}$ in (5) gives $\mathbf{P}_3$ in (2).

Received signal: The elements of the vector $\mathbf{Ps}$ are transmitted in p channel uses. Let n_r denote the number of receive antennas. Let $\mathbf{h}_{(i)}$ denote the $n_r \times 1$ channel vector in the ith channel use, whose entries are the channel gains from the transmit antenna to the receive antennas. The channel gains are modeled as i.i.d. complex Gaussian with zero mean and unit variance. The received signal vector of size $pn_r \times 1$ in p channel uses can be expressed as

$$\mathbf{y} = \mathbf{HPs} + \mathbf{n} = \mathbf{HQAs} + \mathbf{n} = \mathbf{HQx} + \mathbf{n} = \mathbf{Gx} + \mathbf{n}, \quad (6)$$

where $\mathbf{H} = \text{diag}\{\mathbf{h}_{(1)}\ \mathbf{h}_{(2)}\ \cdots\ \mathbf{h}_{(p)}\}$, $\mathbf{P} = \mathbf{QA}$, $\mathbf{x} = \mathbf{As}$, $\mathbf{G} = \mathbf{HQ}$, and $\mathbf{n}$ is the $pn_r \times 1$ noise vector whose entries are modeled as $\mathcal{CN}(0, \sigma^2)$. The ML detection rule for this system model is given by

$$\hat{\mathbf{x}} = \underset{\mathbf{x} \in \mathbb{S}_{n_p,\mathbb{A}}^p}{\text{argmin}}\ \|\mathbf{y} - \mathbf{Gx}\|^2, \quad (7)$$

where $\mathbb{S}_{n_p,\mathbb{A}}^p$ is the set of all possible $\mathbf{x} = \mathbf{As}$ vectors, and $\mathbb{S}_{n_p,\mathbb{A}}$ is given by

$$\mathbb{S}_{n_p,\mathbb{A}} = \{\mathbf{v}_{j,l} : j = 1, \cdots, n_p, \quad l = 1, \cdots, |\mathbb{A}|\},$$
$$\text{s.t.}\ \ \mathbf{v}_{j,l} = [0, \cdots, 0, \underbrace{v_l}_{j\text{th coordinate}}, 0, \cdots, 0]^T, \quad v_l \in \mathbb{A}. \quad (8)$$

For example, for $n_p = 2$ and 4-QAM, $\mathbb{S}_{n_p,\mathbb{A}}$ is given by

$$\mathbb{S}_{2,\text{4-QAM}} = \Bigg\{ \begin{bmatrix} +1+\jmath \\ 0 \end{bmatrix}, \begin{bmatrix} +1-\jmath \\ 0 \end{bmatrix}, \begin{bmatrix} -1+\jmath \\ 0 \end{bmatrix}, \begin{bmatrix} -1-\jmath \\ 0 \end{bmatrix}, \begin{bmatrix} 0 \\ +1+\jmath \end{bmatrix}, \begin{bmatrix} 0 \\ +1-\jmath \end{bmatrix}, \begin{bmatrix} 0 \\ -1+\jmath \end{bmatrix}, \begin{bmatrix} 0 \\ -1-\jmath \end{bmatrix} \Bigg\}. \quad (9)$$

The indices of the non-zero entries in $\hat{\mathbf{x}}$ and the non-zero entries of $\hat{\mathbf{x}}$ are demapped to obtain the information bits. The ML solution in (7) can be computed only for small precoder sizes because of its exponential complexity in p, i.e., $O((|\mathbb{A}|n_p)^p)$). For large precoder sizes, we propose a low complexity detection algorithm in Section IV.

III. Bounds on the capacity of PIM

In this section, we derive upper and lower bounds on the capacity of PIM, where the symbols in the vector $\mathbf{s}$ are from Gaussian codebook. That is, we assume that the transmit vector $\mathbf{s}$ is a Gaussian random vector. The capacity expression for this PIM system can be written as

$$\begin{aligned} C_{PIM} &= \frac{1}{p}\mathbb{E}_{\mathbf{G}}\left(I\left(\mathbf{x};\mathbf{y}\right)\right) \\ &= \frac{1}{p}\mathbb{E}_{\mathbf{G}}\left(h\left(\mathbf{y}\right)-h\left(\mathbf{y}|\mathbf{x}\right)\right) = \frac{1}{p}\mathbb{E}_{\mathbf{G}}\left(h\left(\mathbf{y}\right)-h\left(\mathbf{n}\right)\right) \\ &= \frac{1}{p}\mathbb{E}_{\mathbf{G}}\left(h\left(\mathbf{y}\right)-\log_2\left[\det\left(\pi e\sigma^2\mathbf{I}_{pn_r}\right)\right]\right), \end{aligned} \quad (10)$$

where $h\left(.\right)$ denotes the differential entropy, and $\mathbb{E}_{\mathbf{G}}$ is the expectation of the differential entropy with respect to the random fading channel matrix $\mathbf{G}$. Note that $\mathbf{G}\sim\mathbb{C}\mathcal{N}(0,\sigma^2\mathbf{I}_{pn_r})$. To compute $h\left(\mathbf{y}\right)$ in (10), we require the distribution of $\mathbf{y}$. Define $\mathcal{A}\triangleq\{\mathbf{A}|\mathbf{QA}\in\mathbb{P}\}$. From (6), we can see that the distribution of $\mathbf{y}$ is a Gaussian mixture given by

$$\mathbf{y}\sim\sum_{i=1}^{|\mathbb{P}|}p_i\mathcal{N}\left(\boldsymbol{\mu}_i,\boldsymbol{\Phi}_i\right), \quad (11)$$

$$p_i = \Pr\left(\mathbf{A}^i\right), \mathbf{A}^i\in\mathcal{A}, i=1,\cdots,|\mathbb{P}|, \quad (12)$$

$$\boldsymbol{\mu}_i = \mathbb{E}\left(\mathbf{y}\right)=\mathbb{E}\left(\mathbf{GA}^i\mathbf{s}+\mathbf{n}\right)=\mathbf{0}, \quad (13)$$

$$\begin{aligned} \boldsymbol{\Phi}_i &= \mathbb{E}\left(\mathbf{yy}^H\right)=\mathbb{E}\left[\left(\mathbf{GA}^i\mathbf{s}+\mathbf{n}\right)\left(\mathbf{GA}^i\mathbf{s}+\mathbf{n}\right)^H\right] \\ &= \mathbb{E}\left(\mathbf{GA}^i\mathbf{ss}^H\mathbf{A}^{iH}\mathbf{G}^H\right)+\mathbb{E}\left(\mathbf{nn}^H\right) \\ &= \mathbf{GA}^i\mathbb{E}_{\mathbf{s}}\left(\mathbf{ss}^H\right)\mathbf{A}^{iH}\mathbf{G}^H+\sigma^2\mathbf{I}_{pn_r}. \end{aligned} \quad (14)$$

If all the precoder selection matrices are equally likely, then $p_i=\frac{1}{|\mathbb{P}|}$. when the symbols are independent of each other, $\mathbb{E}_{\mathbf{s}}\left(\mathbf{ss}^H\right)=\sigma_s^2\mathbf{I}_p$, where σ_s^2 is the average signal power per channel use. Now, (11) becomes

$$\mathbf{y}\sim\frac{1}{|\mathbb{P}|}\sum_{i=1}^{|\mathbb{P}|}\mathcal{N}\left(\mathbf{0},\sigma_s^2\mathbf{GA}^i\mathbf{A}^{iH}\mathbf{G}^H+\sigma^2\mathbf{I}_{pn_r}\right). \quad (15)$$

The differential entropy of $\mathbf{y}$ is given by

$$h\left(\mathbf{y}\right)=\frac{-1}{|\mathbb{P}|}\sum_{i=1}^{|\mathbb{P}|}\int_{\mathbf{y}}\mathcal{N}(\mathbf{0},\boldsymbol{\Phi}_i)\log_2\!\left(\frac{1}{|\mathbb{P}|}\sum_{i=1}^{|\mathbb{P}|}\mathcal{N}(\mathbf{0},\boldsymbol{\Phi}_i)\right)d\mathbf{y}. \quad (16)$$

Solving the above expression for a closed-form solution is difficult. Hence, we bound it above and below as follows.

Lower bound, L: Since differential entropy is a concave function, we can write

$$\begin{aligned} h\left(\mathbf{y}\right) &= h\!\left(\frac{1}{|\mathbb{P}|}\sum_{i=1}^{|\mathbb{P}|}\mathcal{N}\left(\mathbf{0},\boldsymbol{\Phi}_i\right)\right) \\ &\geqslant \frac{1}{|\mathbb{P}|}\sum_{i=1}^{|\mathbb{P}|}h\left(\mathcal{N}\left(\mathbf{0},\boldsymbol{\Phi}_i\right)\right) = \frac{1}{|\mathbb{P}|}\sum_{i=1}^{|\mathbb{P}|}\log_2\det\left(\pi e\boldsymbol{\Phi}_i\right) \triangleq l. \end{aligned}$$

From (17), C_{PIM} can be lower bounded as

$$C_{PIM}\geqslant\frac{1}{p}\mathbb{E}_{\mathbf{G}}\left(l-\log_2\left[\det\left(\pi e\sigma^2\mathbf{I}_{pn_r}\right)\right]\right)\triangleq L. \quad (17)$$

Upper bound, U: We approximate the probability distribution of $\mathbf{y}$ to a Gaussian distribution. This gives an upper bound because the entropy of any random variable is bounded above by the entropy of a Gaussian random variable with the same mean and variance. From (14), the mean and covariance of $\mathbf{y}$ are given by

$$\begin{aligned} \mathbb{E}\left(\mathbf{y}\right) &= \mathbf{0} \\ \mathbb{E}\left(\mathbf{yy}^H\right) &= \mathbf{G}\mathbb{E}_{\mathbf{A}}\left[\mathbf{A}^i\mathbb{E}_{\mathbf{s}}\left(\mathbf{ss}^H\right)\mathbf{A}^{iH}\right]\mathbf{G}^H+\sigma^2\mathbf{I}_{pn_r} \\ &= \mathbf{G}\left(\frac{1}{|\mathbb{P}|}\sum_{i=1}^{|\mathbb{P}|}\mathbf{A}^i\left(\sigma_s^2\mathbf{I}_p\right)\mathbf{A}^{iH}\right)\mathbf{G}^H+\sigma^2\mathbf{I}_{pn_r} \\ &= \frac{\sigma_s^2}{|\mathbb{P}|}\mathbf{G}\left(\sum_{i=1}^{|\mathbb{P}|}\mathbf{D}^i\right)\mathbf{G}^H+\sigma^2\mathbf{I}_{pn_r}, \end{aligned} \quad (18)$$

where $\mathbf{D}^i=\mathbf{A}^i\mathbf{A}^{iH}$. Let $\left\{I_1^i,I_2^i,...I_p^i\right\}$ be the set of column indices in $\mathbf{Q}$ that corresponding to the precoder selection matrix $\mathbf{A}^i$. It can then be seen that $\mathbf{D}^i$ is a diagonal matrix such that

$$\left(\mathbf{D}^i\right)_{j,k} = \begin{cases}1, & \text{if } j=k=I\in\left\{I_1^i,I_2^i,...I_p^i\right\}\\ 0, & \text{otherwise,}\end{cases} \quad (19)$$

where $\left(\mathbf{D}^i\right)_{j,k}$ is the element in the ith row and jth column of $\mathbf{D}^i$. Since the total number of precoder selection matrices is $|\mathbb{P}|=2^{np}$, the number of times any particular column in $\mathbf{Q}$ will be chosen is $2^{n(p-1)}$. Therefore, $\sum_{i=1}^{|\mathbb{P}|}\mathbf{D}^i=2^{n(p-1)}\mathbf{I}_{pn_p}$ and (18) becomes

$$\begin{aligned} \mathbb{E}\left(\mathbf{yy}^H\right) &= \frac{\sigma_s^2}{2^{np}}\mathbf{G}\left(2^{n(p-1)}\mathbf{I}_{pn_p}\right)\mathbf{G}^H+\sigma^2\mathbf{I}_{pn_r} \\ &= \frac{\sigma_s^2}{2^n}\mathbf{GG}^H+\sigma^2\mathbf{I}_{pn_r}\triangleq\boldsymbol{\Phi}'. \end{aligned} \quad (20)$$

Thus, an upper bound on the PIM capacity is given by

$$\begin{aligned} C_{PIM} &\leqslant \frac{1}{p}\mathbb{E}_{\mathbf{G}}\left(\log_2\det\left(\pi e\boldsymbol{\Phi}'\right)-\log_2\det\left(\pi e\sigma^2\mathbf{I}_{pn_r}\right)\right) \\ &= \frac{1}{p}\mathbb{E}_{\mathbf{G}}\left(\log_2\det\left(\frac{\sigma_s^2}{\sigma^2 2^n}\mathbf{GG}^H+\mathbf{I}_{pn_r}\right)\right)\triangleq U. \end{aligned} \quad (21)$$

Numerical results: In Fig. 2, we plot the lower and upper bounds on the PIM capacity as a function of SNR for $p=6$, $n=1$, and $n_r=1$. The lower bound L is computed using (17) and the upper bound U is computed using (21). In Fig. 2, we observe that the gap between upper and lower bounds $U-L=0.09$ bps/Hz at 0 dB SNR. At 40 dB SNR, the gap between the bounds is 1 bps/Hz. Also, the normalized gap, given by $\frac{U-L}{U}$, is 0.11 for 0 dB SNR and 0.08 for 40 dB SNR. This illustrates that the derived bounds are fairly tight.

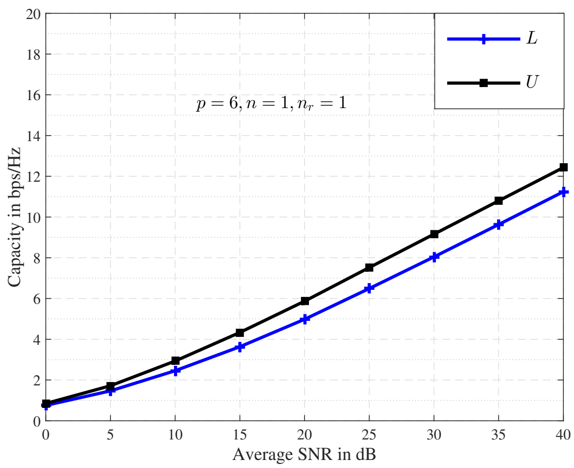

Fig. 2. Lower and upper bounds on the capacity of PIM for $p = 6$, $n = 1$, and $n_r = 1$.

IV. MESSAGE PASSING DETECTION FOR PIM

ML detection of PIM signals with large precoder sizes is prohibitive because of the exponential complexity in the precoder size. Therefore, in this section, we propose a low complexity message passing based algorithm suited for detection of PIM signals with large precoder sizes. Towards this, we model the system using a fully connected factor graph with p variable (or factor) nodes and pn_r observation nodes. The variable nodes corresponding to $\mathbf{x}_k$s, $k = 1, \cdots, p$, and observation nodes corresponding to y_is, $i = 1, \cdots, pn_r$, are shown in Fig. 3(a). Message passing over this graphical model gives us an approximate solution to the maximum a posteriori probability distribution of the variable nodes $\mathbf{x}_k$s.

Messages: We derive the messages passed in the factor graph as follows. Equation (6) can be written as

$$y_i = \mathbf{g}_{i,[k]}\mathbf{x}_k + \sum_{j=1, j\neq k}^{p} \mathbf{g}_{i,[j]}\mathbf{x}_j + n_i, \quad i = 1, \cdots, pn_r, \quad (22)$$

where $\mathbf{g}_{i,[j]}$ is a row vector of length n_p, given by $[G_{i,(j-1)n_p+1} \;\; G_{i,(j-1)n_p+2} \;\; \cdots \;\; G_{i,jn_p}]$, and $\mathbf{x}_j \in \mathbb{S}_{n_p,\mathbb{A}}$. Since the transmitted value of $\mathbf{x}_k$ is unknown at the receiver, we model $\mathbf{x}_k$ as a random vector with mean $\mathbf{u} \in \mathbb{S}_{n_p,\mathbb{A}}$ and variance Var($\mathbf{g}_{i,[k]}\mathbf{x}_k|y_i$). Thus, we can write

$$\mathbf{x}_k = \mathbf{u} + \tilde{\mathbf{x}}_k, \quad (23)$$

where $\mathbf{u}$ is a deterministic vector from $\mathbb{S}_{n_p,\mathbb{A}}$ and $\tilde{\mathbf{x}}_k$ is a random vector with mean zero and variance equal to the variance of $\mathbf{g}_{i,[k]}\mathbf{x}_k$ conditioned on y_i and evaluated from the current estimate of p_{ki}, i.e.,

$$\begin{aligned}\text{Var}\big(\mathbf{g}_{i,[k]}\tilde{\mathbf{x}}_k\big) &= \text{Var}\left(\mathbf{g}_{i,[k]}\mathbf{x}_k|y_i\right) \\ &= \sum_{\mathbf{v}\in\mathbb{S}_{n_p,\mathbb{A}}} p_{ki}(\mathbf{v})\big|\mathbf{g}_{i,[k]}\mathbf{v}\big|^2 - \Big|\sum_{\mathbf{v}\in\mathbb{S}_{n_p,\mathbb{A}}} p_{ki}(\mathbf{v})\mathbf{g}_{i,[k]}\mathbf{v}\Big|^2, \end{aligned} \quad (24)$$

where $p_{ki}(\mathbf{u})$ is the message from kth variable node to the ith observation node. Substituting (23) into (22) yields

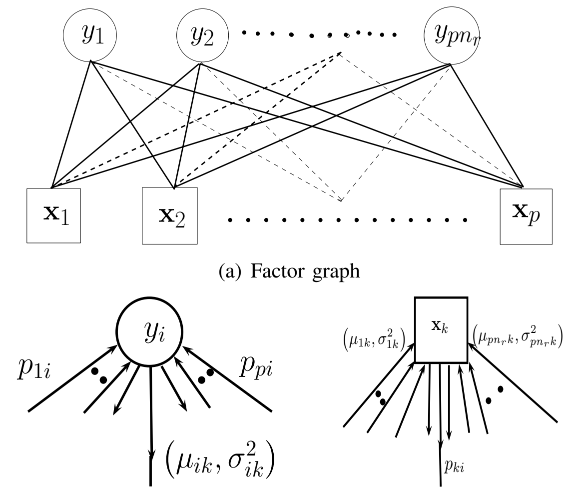

(a) Factor graph

(b) Observation node messages (c) Variable node messages

Fig. 3. The factor graph and messages passed in the proposed algorithm.

$$y_i = \mathbf{g}_{i,[k]}\mathbf{u} + \underbrace{\mathbf{g}_{i,[k]}\tilde{\mathbf{x}}_k + \sum_{j=1,j\neq k}^{p} \mathbf{g}_{i,[j]}\mathbf{x}_j + n_i}_{\triangleq\, z_{ik}}, \quad (25)$$

We approximate the term z_{ik} to have a Gaussian distribution with mean μ_{ik} and variance σ^2_{ik} as follows:

$$\begin{aligned}\mu_{ik} &= \mathbb{E}\Big[\mathbf{g}_{i,[k]}\tilde{\mathbf{x}}_k + \sum_{j=1,j\neq k}^{p} \mathbf{g}_{i,[j]}\mathbf{x}_j + n_i\Big] \\ &= \sum_{j=1,j\neq k}^{p} \sum_{\mathbf{v}\in\mathbb{S}_{n_p,\mathbb{A}}} p_{ji}(\mathbf{v})\mathbf{g}_{i,[j]}\mathbf{v}, \end{aligned} \quad (26)$$

$$\sigma^2_{ik} = \text{Var}\Big(\mathbf{g}_{i,[k]}\tilde{\mathbf{x}}_k + \sum_{j=1,j\neq k}^{p} \mathbf{g}_{i,[j]}\mathbf{x}_j + n_i\Big)$$

$$= \sum_{j=1}^{p} \sum_{\mathbf{v}\in\mathbb{S}_{n_p,\mathbb{A}}} p_{ji}(\mathbf{v})\big|\mathbf{g}_{i,[j]}\mathbf{v}\big|^2 - \Big|\sum_{\mathbf{v}\in\mathbb{S}_{n_p,\mathbb{A}}} p_{ji}(\mathbf{v})\mathbf{g}_{i,[j]}\mathbf{v}\Big|^2 + \sigma^2. \quad (27)$$

The message $p_{ki}(\mathbf{u})$ is given by

$$p_{ki}(\mathbf{u}) \propto \prod_{m=1,m\neq i}^{pn_r} \frac{1}{\sigma_{mk}} \exp\Big(-\frac{\big|y_m - \mu_{mk} - \mathbf{g}_{m,[k]}\mathbf{u}\big|^2}{2\sigma^2_{mk}}\Big). \quad (28)$$

The Gaussian approximation helps us to reduce the complexity of computation of the messages. Further, this approximation is reasonably accurate at large dimensions.

Message passing: The message passing is done as follows.
Step 1: Initialize $p_{ki}(\mathbf{u})$ to $1/|\mathbb{S}_{n_p,\mathbb{A}}|$ for all i, k and $\mathbf{u}$.
Step 2: Compute μ_{ik} and σ^2_{ik} from (26) and (27), respectively.
Step 3: Compute p_{ki} from (28). In (28) use damping [12] of the messages to improve the convergence rate with a damping factor $\delta \in (0, 1]$.
Repeat Steps 2 and 3 for a certain number of iterations. Figures 3(b) and 3(c) illustrate the exchange of messages between observation and variable nodes, where the vector message $\mathbf{p}_{ki} = [p_{ki}(\mathbf{u}_1), p_{ki}(\mathbf{u}_2), \cdots, p_{ki}(\mathbf{u}_{|\mathbb{S}_{n_p,\mathbb{A}}|})]$. The final symbol probabilities at the end are given by

$$p_k(\mathbf{u}) \propto \prod_{m=1}^{pn_r} \frac{1}{\sigma_{mk}} \exp\Big(-\frac{\big|y_m - \mu_{mk} - \mathbf{g}_{m,[k]}\mathbf{u}\big|^2}{2\sigma^2_{mk}}\Big). \quad (29)$$

Input: $\mathbf{y}$, $\mathbf{G}$, σ^2
Initialize: $p_{ki}^{(0)}(\mathbf{u}) \leftarrow 1/|\mathbb{S}_{n_p,\mathbb{A}}|$, $\forall i,k,\mathbf{u}$
for $t = 1 \rightarrow number\_of\_iterations$ **do**
  for $i = 1 \rightarrow pn_r$ **do**
    for $j = 1 \rightarrow p$ **do**
      $\tilde{\mu}_{ij} \leftarrow \sum_{\mathbf{v}\in\mathbb{S}_{n_p,\mathbb{A}}} p_{ji}^{(t-1)}(\mathbf{v})\mathbf{g}_{i,[j]}\mathbf{v}$
    end
    $\mu_i \leftarrow \sum_{j=1}^{p} \tilde{\mu}_{ij}$
    $\sigma_i^2 \leftarrow \sum_{j=1}^{p} \sum_{\mathbf{v}\in\mathbb{S}_{n_p,\mathbb{A}}} p_{ji}^{(t-1)}(\mathbf{v})\left|\mathbf{g}_{i,[j]}\mathbf{v}\right|^2 - \left|\tilde{\mu}_{ij}\right|^2 + \sigma^2$
    for $k = 1 \rightarrow p$ **do**
      $\mu_{ik} \leftarrow \mu_i - \tilde{\mu}_{ik}$
      $\sigma_{ik}^2 \leftarrow \sigma_i^2$
    end
  end
  for $k = 1 \rightarrow p$ **do**
    for $i = 1 \rightarrow pn_r$ **do**
      foreach $\mathbf{u} \in \mathbb{S}_{n_p,\mathbb{A}}$ **do**
        $\tilde{p}_{ki}(\mathbf{u}) \leftarrow - \sum_{\substack{m=1\\m\neq i}}^{pn_r} \ln(\sigma_{mk}) + \frac{\left|y_m - \mu_{mk} - \mathbf{g}_{m,[k]}\mathbf{u}\right|^2}{2\sigma_{mk}^2}$
        $p_{ki}^{(t)}(\mathbf{u}) = \frac{(1-\delta)}{C_{ki}} \exp(\tilde{p}_{ki}^{(t)}(\mathbf{u})) + \delta p_{ki}^{(t-1)}(\mathbf{u})$
        ($C_{ki}$is a normalizing constant)
      end
    end
  end
end
Output: $p_k(\mathbf{u})$ as per (29) and $\hat{\mathbf{x}}_k$ as per (30), $\forall k$

Algorithm 1: Listing of the proposed detection algorithm.

The detected vector $\hat{\mathbf{x}}_k$ at the receiver is obtained as

$$\hat{\mathbf{x}}_k = \underset{\mathbf{u}\in\mathbb{S}_{n_p,\mathbb{A}}}{\text{argmax}} \ p_k(\mathbf{u}). \tag{30}$$

The non-zero entries in $\hat{\mathbf{x}}_k$s and its indices are then demapped to obtain the information bits. The algorithm listing is given in **Algorithm 1**. The total complexity of this proposed detection algorithm is $O(p^2 n_r n_p |\mathbb{A}|)$, which is quadratic in p.

Simulation results: In Fig. 4, we show the BER performance of PIM system with $n = 1$, BPSK, $n_r = 2$, for different precoder sizes ($p = 10, 20, 30, 150$) using the proposed detection algorithm, obtained through simulations. The system throughput is 2 bpcu (1 bit through precoder indexing and 1 bit through BPSK modulation). The number of iterations used in the detection algorithm is 15 and the damping factor used is $\delta = 0.3$. It can be observed that the performance of the algorithm is poor for small p. But as p gets large, the performance improves. This is because the Gaussian approximation used in the forming the messages becomes more and more accurate, resulting in increasingly better performance for increasing p. For example, with $p = 150$, it achieves 10^{-5} BER at just 10 dB SNR. This good performance is due to the diversity benefit offered by the PRPP matrices.

V. Enhanced Precoder index modulation

In this section, we propose an enhanced PIM (E-PIM) scheme which provides additional signaling support to the

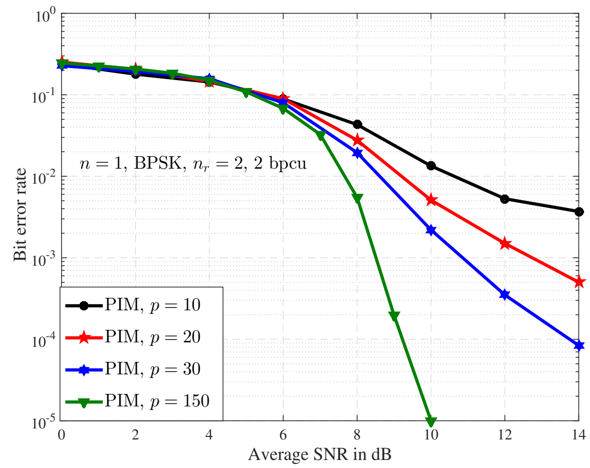

Fig. 4. BER performance of the proposed detection algorithm in PIM system with $n = 1$, BPSK, $n_r = 2$, 2 bpcu, and $p = 10, 20, 30, 150$.

index bits, but without loosing spectral efficiency compared to PIM. The matrix $\mathbf{Q}$, precoder selection matrix $\mathbf{A}$, and precoder set $\mathbb{P}$ are defined as in Section II.

The proposed E-PIM transmitter is shown in Fig. 5. The E-PIM transmitter takes $\lfloor\log_2|\mathbb{P}|\rfloor + p\lfloor\log_2|\mathbb{A}|\rfloor$ bits and encodes them as follows. The $p\lfloor\log_2|\mathbb{A}|\rfloor$ bits are used to obtain p modulation symbols. Let $\mathbf{s} \in \mathbb{A}^p$ denote the vector of these modulation symbols. $\lfloor\log_2|\mathbb{P}|\rfloor$ bits are used to construct $pn_p \times p$ precoder selection matrix $\mathbf{A}$ to select precoder matrix $\mathbf{P}$ from precoder set $\mathbb{P}$ such that $\mathbf{P} = \mathbf{QA} \in \mathbb{P}$. The modulation symbol vector $\mathbf{s}$ is then precoded using $p \times p$ precoder matrix $\mathbf{P}$ to get the vector $\mathbf{Ps}$. Transmission in E-PIM is done as follows.

Let $\mathbf{b}$ be a $1 \times n_p$ phase vector whose ith element is given by $e^{\jmath\frac{2(i-1)\pi}{n_p}}$, $i = 1, \cdots, n_p$, i.e.,

$$\mathbf{b} = \left[e^{\jmath 0} \ e^{\jmath\frac{2\pi}{n_p}} \ e^{\jmath\frac{4\pi}{n_p}} \ \cdots \ e^{\jmath\frac{2(n_p-1)\pi}{n_p}} \right]. \tag{31}$$

Note that $\mathbf{ba}_{(i)} = e^{\jmath\frac{2\pi}{n_p}(j_i-1)}$, where $\mathbf{a}_{(i)}$ is given in (4). Let $(\mathbf{Ps})_i$ denote the ith element of $\mathbf{Ps}$. In PIM, $(\mathbf{Ps})_i$ is transmitted as such in the ith channel use. Whereas, in E-PIM, $\mathbf{ba}_{(i)}(\mathbf{Ps})_i$ is transmitted in the ith channel use. By doing so, we are essentially providing additional signaling support to index bits through $\mathbf{ba}_{(i)}$ in addition to the support through $\mathbf{P}$. Whereas, PIM provides signaling support to index bits only through $\mathbf{P}$. Note that the number of index bits and modulation bits sent per channel use in E-PIM is the same as that in PIM. The additional support in E-PIM provided through $\mathbf{ba}_{(i)}$ improves the reliability of the index bits. This results in improved performance in E-PIM compared to PIM.

Received signal: The received signal vector of size $pn_r \times 1$ in p channel uses can be expressed as

$$\mathbf{y} \ = \ \mathbf{HBAPs} + \mathbf{n} \ = \ \mathbf{HBAQAs} + \mathbf{n}, \tag{32}$$

where $\mathbf{B} = \text{diag}\{\mathbf{b}, \mathbf{b}, \cdots \mathbf{b}\}$ is the $p \times pn_p$ support phase matrix. The ML detection rule for this system is given by

$$\{\hat{\mathbf{s}}, \hat{\mathbf{A}}\} = \underset{\mathbf{s}\in\mathbb{A}^p, \forall\mathbf{A}}{\text{argmin}} \ \|\mathbf{y} - \mathbf{HBAQAs}\|^2. \tag{33}$$

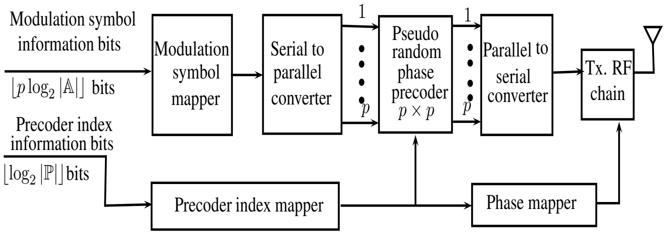

Fig. 5. E-PIM transmitter.

The indices of the non-zero rows in $\hat{\mathbf{A}}$ and the entries of $\hat{\mathbf{s}}$ are demapped to obtain the information bits.

Simulation results: In Figs. 6 and 7, we present the BER performance of the proposed E-PIM scheme obtained through simulations. The BER performance of PIM for the same system parameter settings is also shown for comparison. ML detection is used for both PIM and E-PIM. In Fig. 6, the modulation used is 4-QAM and bpcu is 3. In Fig. 7, the modulation used is 8-QAM and bpcu is 4. The following system parameters are used: $n = 1$, $n_r = 1$, and $p = 3, 4, 5$. From Figs. 6 and 7, we can see that E-PIM performs better than PIM. For example, for $p = 4$, E-PIM performs better by about 1 dB at 10^{-3}. As mentioned before, this performance improvement is due to the improved reliability of the index bits in E-PIM realized through additional signaling support for the index bits .

VI. Conclusions

Precoder index modulation is a promising modulation scheme proposed recently. It uses the idea of indexing precoder matrices for conveying additional information bits. In this paper, we made the following new contributions in the area of precoder index modulation. First, we derived lower and upper bounds on the capacity of PIM, which have not been reported before. Second, to enable the detection of PIM signals with large precoder sizes, we proposed a low complexity detection algorithm based on message passing. Simulation results showed that the proposed algorithm achieved very good performance for large precoder sizes. Third, we also proposed an enhanced PIM (E-PIM) scheme which achieved better performance compared to the basic PIM scheme. In this work we have considered low complexity detection of PIM signals with BPSK in a point-to-point setting. Low complexity detection of PIM signals with higher-order modulation in multiuser settings can be taken up for future work.

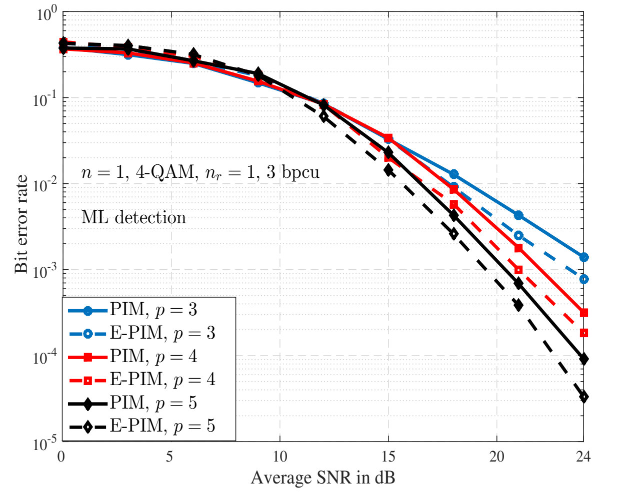

Fig. 6. BER performance comparison between PIM and E-PIM with $n = 1$, 4-QAM, $n_r = 1$, 3 bpcu, $p = 3, 4, 5$, and ML detection.

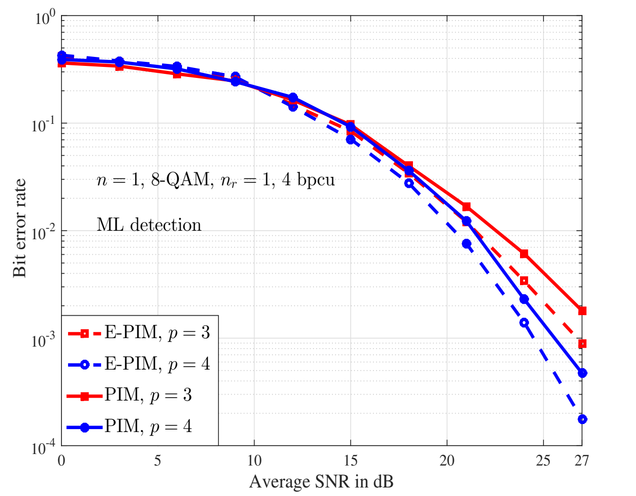

Fig. 7. BER performance comparison between PIM and E-PIM with $n = 1$, 8-QAM, $n_r = 1$, 4 bpcu, $p = 3, 4$, and ML detection.

References

[1] M. Di Renzo, H. Haas, A. Ghrayeb, S. Sugiura, and L. Hanzo, “Spatial modulation for generalized MIMO: challenges, opportunities and implementation,” *Proceedings of the IEEE*, vol. 102, no. 1, pp. 53-55, Jan. 2014.

[2] A. Chockalingam and B. Sundar Rajan, *Large MIMO Systems*, Cambridge Univ. Press, Feb. 2014.

[3] R. Abu-alhiga and H. Haas, “Subcarrier-index modulation OFDM,” *Proc. IEEE PIMRC’2009*, pp. 177-181, Sep. 2009.

[4] E. Basar, U. Aygolu, E. Panayirci, and H. V. Poor, “Orthogonal frequency division multiplexing with index modulation,” *Proc. IEEE GLOBECOM’2012*, pp. 4741-4746, Dec. 2012.

[5] T. Datta, H. Eshwaraiah, and A. Chockalingam, “Generalized space and frequency index modulation,” to appear in *IEEE Trans. Veh. Tech.*, 2015. Available online: arXiv:1506.08291 [cs.IT] 27 Jun 2015.

[6] N. Serafimovski1, S. Sinanovic, M. Di Renzo, and H. Haas, “Multiple access spatial modulation,” *EURASIP J. Wireless Commun. and Networking 2012*, 2012:299.

[7] T. Lakshmi Narasimhan, P. Raviteja, and A. Chockalingam, “Generalized spatial modulation in large-scale multiuser MIMO systems,” *IEEE Trans. Wireless Commun.*, vol. 14, no. 7, pp. 3764-3779, Jul. 2015.

[8] T. Lakshmi Narasimhan, Y. Naresh, T. Datta, and A. Chockalingam, “ Pseudo-random phase precoded spatial modulation and precoder index modulation, ” *Proc. IEEE GLOBECOM’2014,* pp. 3868 - 3873, Dec. 2014.

[9] R. Annavajjala and P. V. Orlik, “Achieving near exponential diversity on uncoded low-dimensional MIMO, multi-user and multi-carrier systems without transmitter CSI,” *Proc. ITA’2011*, Jan. 2011.

[10] M. Pajovic, K. J. Kim, T. Koike-Akino, and P. V. Orlik, “ Modified probabilistic data association algorithms,” *Proc. IEEE ICC’2014*, pp. 5628-5634, Jun. 2014.

[11] T. Lakshmi Narasimhan and A. Chockalingam, “Precoder index modulation,” available online: arXiv:1407.1487v1 [cs.IT] 6 Jul 2014.

[12] M. Pretti, “A message passing algorithm with damping,” *J. Stat. Mech.: Theory and Practice*, Nov. 2005.